Electronic Supplementary Material (ESI) for ChemComm.
This journal is © The Royal Society of Chemistry 2022

Supporting Information

Intercalation-induced amorphous hydrated vanadium oxide for boosted aqueous Zn^{2+} storage

*Duo Chen *[ab]†, Boran Wang [c]†, Xueliang Cui[a], Hang Yang [b], Mengjie Lu [b], Dong Cai [d], Wei Han*[b]*

[a] *Jiangsu Key Laboratory of Electrochemical Energy Storage Technologies, College of Materials Science and Technology, Nanjing University of Aeronautics and Astronautics, Nanjing 210016, China. E-mail: chenduo@nuaa.edu.cn*

[b] *College of Physics, State Key Laboratory of Inorganic Synthesis and Preparative Chemistry, International Center of Future Science, Jilin university, Changchun, 130012, P.R. China. E-mail: whan@jlu.edu.cn*

[c] *Shenzhen Geim Graphene Center, Tsinghua-Berkeley Shenzhen Institute & Tsinghua Shenzhen International Graduate School, Tsinghua University, Shenzhen, 518055 P. R. China*

[d] *Key Laboratory of Carbon Materials of Zhejiang Province, Wenzhou University, Wenzhou, 325035, P.R. China.*

† These authors contributed equally to this work.

Methods

Synthesis of MgVOH and VOH electrodes. The MgVOH electrode was prepared via a facile one-step solvent evaporation method. Typically, 0.5 g V_2O_5 and 0.24 g $MgCl_2$ were dissolved into 40 mL solution of 1 M HCl with continuous stirring for 6 h. Then hydrophilic carbon papers were put into the solution with proper amount, which was subsequently dried in the in fuming cupboard overnight. Lastly, after rinse using deionized water to remove the residual $MgCl_2$, the Mg^{2+}-inserted hydrated vanadium oxide was obtained, denoted as MgVOH. The mass loading of the self-standing MgVOH electrode was 3-5 mg cm^{-2}. And the layered VOH electrode was synthesized via the similar method except without the addition of $MgCl_2$.

Characterization. XRD was conducted by a Rigaku Smart-Lab X-ray diffractometer to analyze the phase and crystalline structure of materials. Scanning electron microscopy (SEM, Regulus 8100) and transmission electron microscopy (TEM, JEOL JSM-2010F) were employed to investigate morphology characterization. X-Ray photoelectron spectroscopy (XPS) was carried out using a Thermo Escalab 250Xi electron spectrometer.

Device assembly and electrochemical measurements. The coin-type cells were assembled using the MgVOH as cathode, Zn foil as anode, 2 M $ZnSO_4$ as electrolyte and glass fiber paper (Whatman GF/D) as separator. As for quasi-solid-state pouch cells, a low-cost PAM/$ZnSO_4$ gel was used as both electrolyte and separator, and the battery was sealed by Al-plastic film. The CV curves were tested via a CHI760E electrochemical working station. And the galvanostatic cycling studies and GITT test were carried out by the LAND CT21001A device.

As for the PAM/$ZnSO_4$ gel electrolyte, monomer (4 g of acrylamide), initiator (30 mg of $K_2S_2O_8$), and cross-linker (4 mg of N,N'-methylenebis-(acrylamide)) were first mixed in 20 mL of deionized water. After a polymerization process at 40 ℃ for 4 h, the gel film was further soaked in 2 M $ZnSO_4$ solution for 48 h. At last, the PAM/$ZnSO_4$ gel electrolyte was obtained.

Galvanostatic intermittence titration technique (GITT). The diffusion coefficient (D_{Zn}) was determined based on the followed equation:

$$D = \frac{4L^2}{\pi\tau}\left(\frac{\Delta E_s}{\Delta E_t}\right)^2 \qquad (1)$$

where τ refers to duration time (s) of the current pulse, L represents the Zn^{2+} diffusion length (cm, that is equal to the thickness of active material), ΔE_s corresponds to the steady-state potential change (V) caused by the current pulse, and ΔE_t is the direct change of voltage (V) before relaxation. In this measurement, current pulse of 0.1 A g^{-1} was applied for 600 s and the relaxation time was 1800 s.

Supporting Figures

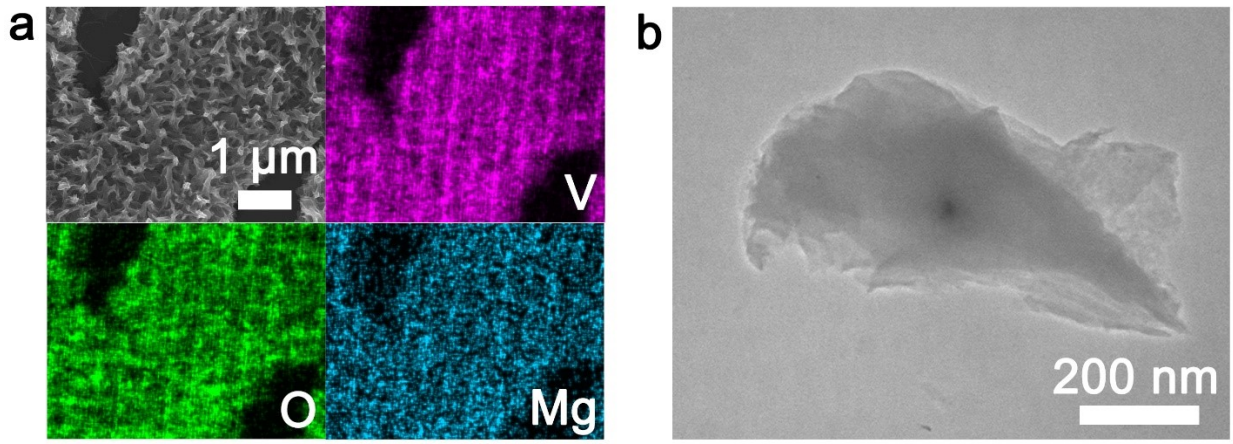

Fig. S1. a) Element mappings, and b) TEM images of the layered MgVOH.

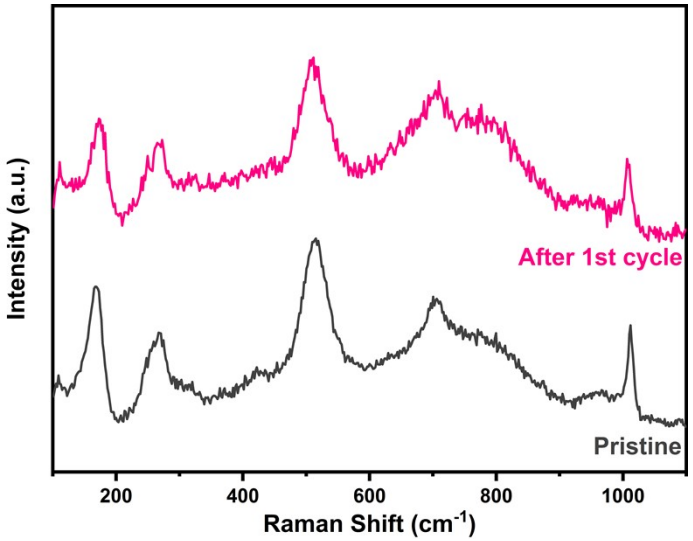

Fig. S2. Raman spectra of the MgVOH electrode in the pristine state and after the 1st cycle.

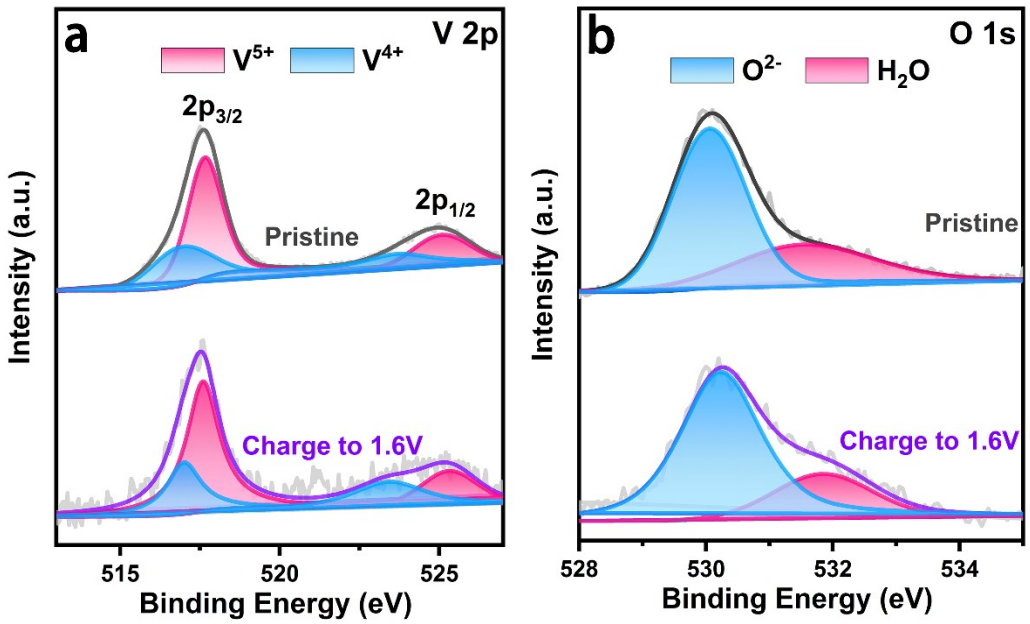

Fig. S3. XPS spectra of the MgVOH electrode in the pristine and fully charged states.

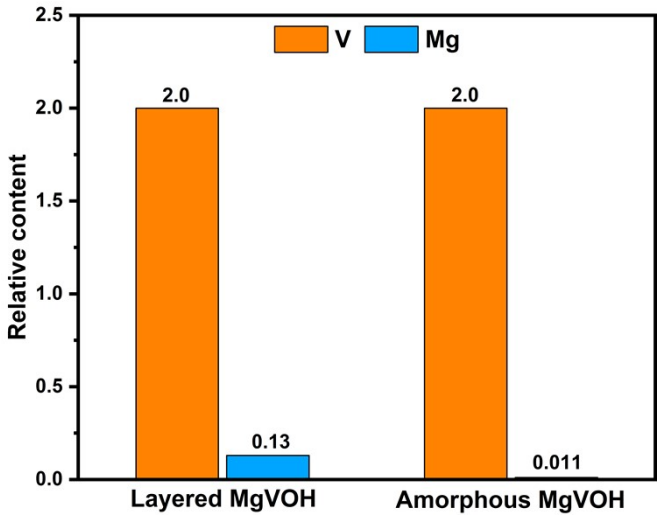

Fig. S4. The relative content between Mg and V in the pristine layered MgVOH and intercalation-induced amorphous MgVOH after the 1st cycle. The initial MgVOH electrode can be determined as $Mg_{0.13}V_2O_5 \cdot nH_2O$. It turns into amorphous structure after the 1st cycle, and the chemical composition of the amorphous MgVOH can be denoted as $Mg_{0.01}V_2O_5 \cdot nH_2O$.

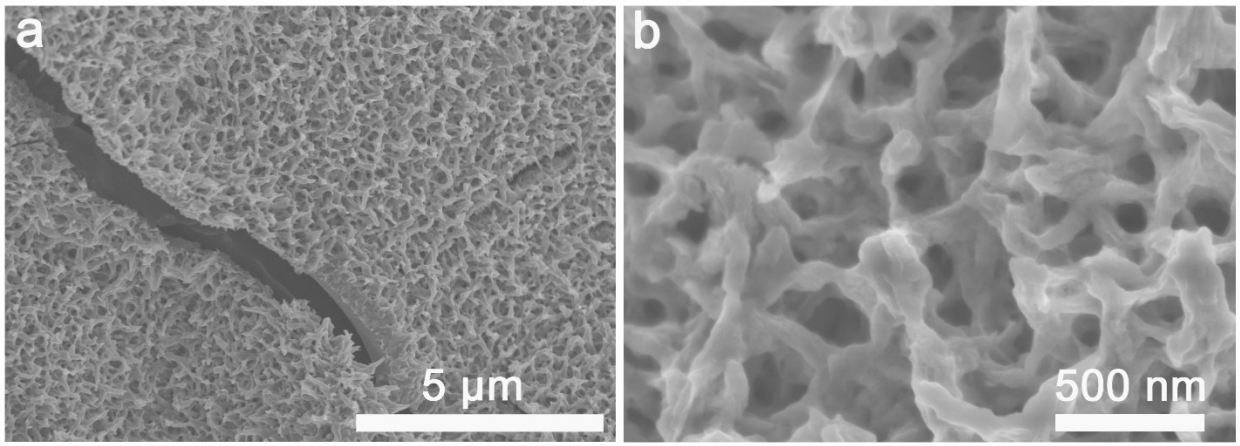

Fig. S5. SEM images in different magnifications for the amorphous MgVOH electrode.

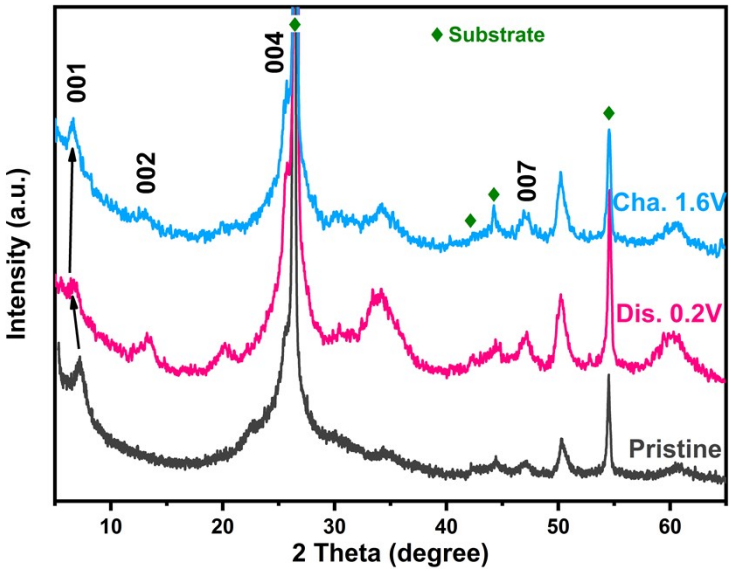

Fig. S6. XRD patterns for the VOH electrode in different discharges/charged states.

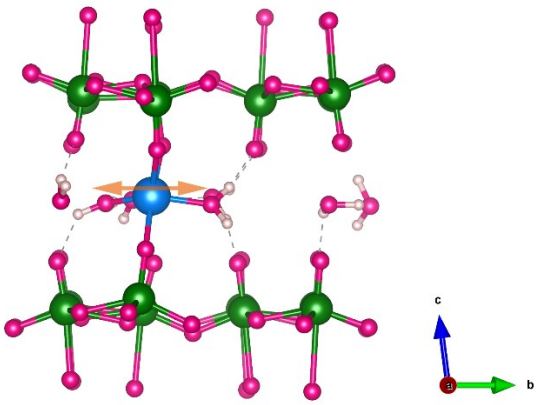

Fig. S7. Optimized structure diagram of MgVOH for analyzing its atom vibration information and potential crystal stability. A micro disturbance along 66 different orientations is respectively applied on the Mg atom to simulate its vibration information. Calculated results can be available from Table S1.

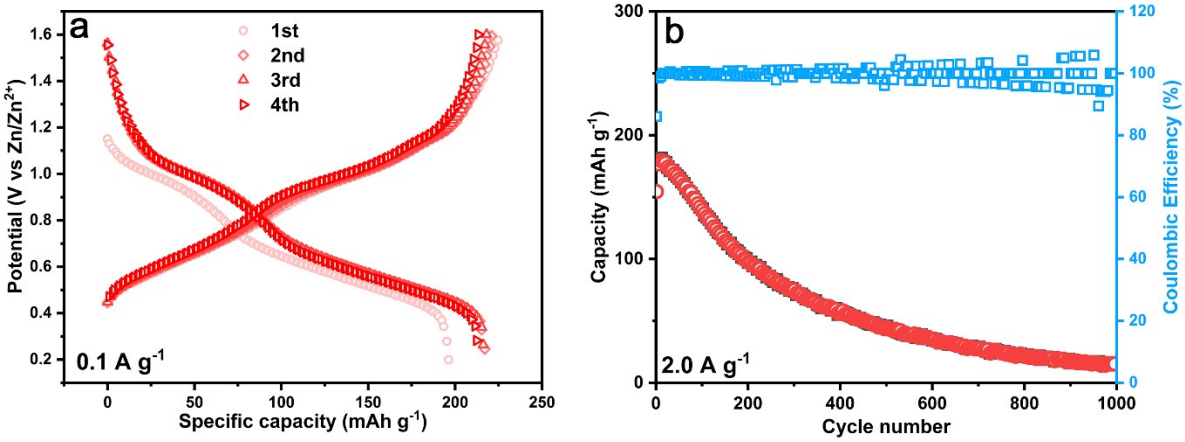

Fig. S8. Electrochemical properties of the layered VOH cathode. a) Discharge/charge profiles at 0.1 A g^{-1}. b) Cycling stability test at 2.0 A g^{-1}.

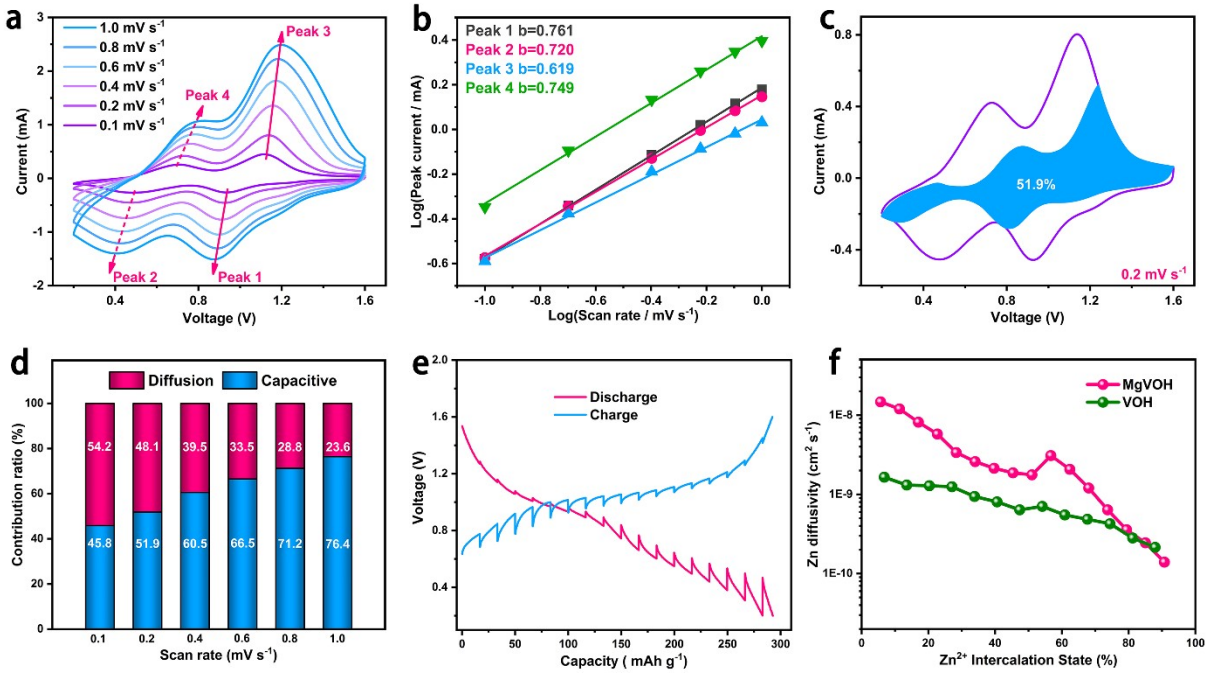

Fig. S9 Electrochemical kinetics of MgVOH electrodes. a) CV curves at various scan rates from 0.1 to 1.0 mV s^{-1}. b) Log(peak current) versus Log(scan rate) plots according to the four peaks in a). c) Capacitive contribution at 0.2 mV s^{-1}. d) Capacity contribution at different scan rates. e) The charge/discharge profiles in the GITT measurement. f) The comparison of the calculated Zn^{2+} diffusivity coefficient between MgVOH and VOH cathodes.

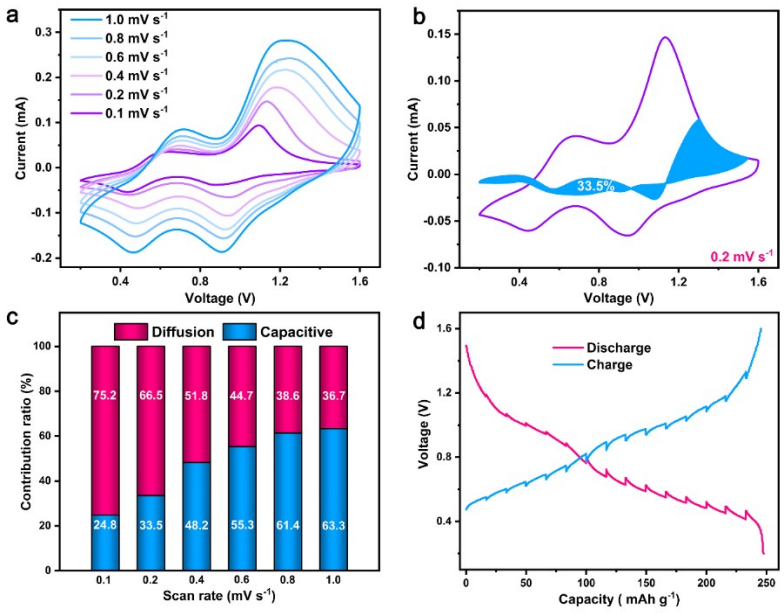

Fig. S10. Electrochemical kinetics analyses for VOH electrode. a) CV curves recorded at different scan rates from 0.1 to 1.0 mV s^{-1}. b) Capacitive contribution at 0.2 mV s^{-1}. c) Contribution ratio for diffusion-controlled and capacitive capacity at various scan rates. d) The charge/discharge profiles in the GITT measurement for the VOH electrode.

Supplementary Note 1:

The electrochemical kinetics for the amorphous MgVOH is probed via CV measurements conducted at various scan rates from 0.1 to 1.0 mV s^{-1}. As seen in **Fig. S8**a, all curves exhibit similar shapes with four redox peaks, demonstrating the electrochemical behavior for MgVOH is well reserved even at large scan rate. The peak current (i) and corresponding scan rate (v) have been known to observe a power law of $i = av^b$, where the b value of 0.5 is considered as a diffusion-controlled faradic process, while the b value of 1.0 implies a surface-induced pseudocapacitive contribution [49, 50]. The b values for MgVOH can be determined by the fitting lines in **Fig. S8**b, in which the values for the four peaks are 0.761, 0.720, 0.619 and 0.749, respectively. It reveals that the charge storage process may be a result of the combined effect from the diffusion-controlled and the pseudocapacitance reaction. Moreover, the capacity contribution can be quantitatively calculated by the equation of $i_{(U)} = k_1 v + k_2 v^{1/2}$, where the factor k_1 and k_2 refer to the ratio of the current response from capacitive and diffusion-controlled behavior at a fixed potential (U), respectively [50]. **Fig. S8**c displays the typical CV curve at 0.2 mV s^{-1} with a separated surface-induced capacitive current (cyan region), which accounts for 51.9% of the total contribution. When the scan rate increases from 0.1 to 1.0 mV s^{-1}, the capacitive contribution of MgVOH rises from 45.8% to 76.4% (**Fig. S8**d), which is higher than the VOH electrode (as shown in **Fig. S9**), implying a faster charge transfer kinetics of amorphous MgVOH [32]. Furthermore, we also conducted the galvanostatic intermittent titration technique (GITT) to investigate the Zn^{2+} solid-state diffusion in the cathode materials. The typical discharge/charge profiles and the calculated Zn^{2+} diffusion coefficient (D_{Zn}) are shown in **Fig. S8**e,f and **Fig. S9d** (details of test and calculation are available in Supplementary Information). The D_{Zn} value for MgVOH electrode is in the magnitude of 10^{-10} to 10^{-8}, which is higher than VOH cathode benefitting from the more isotropic Zn-ion diffusion routes in the amorphous MgVOH.

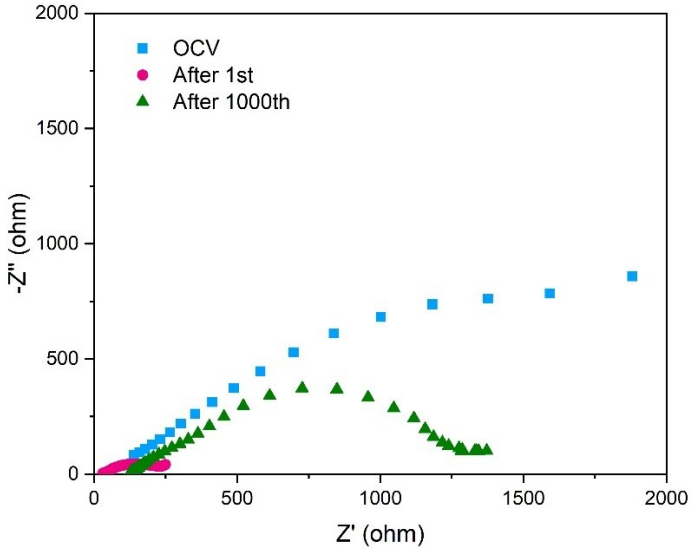

Fig. S11. Nyquist plots of MgVOH cathode at different cycling stages.

Supplementary Note 2:

The electrochemical impedance spectroscopy (EIS) analysis of MgVOH cathode could exhibit the evolution of charge transfer resistance (R_{CT}). It can be seen that R_{CT} of MgVOH reduces substantially after the 1st cycle owing to the activation and phase transition of the pristine electrode at the first cycle. And the resistance increases after 1000 cycles, which might be caused by the tardy phase transformation from amorphous MgVOH to ZOV.

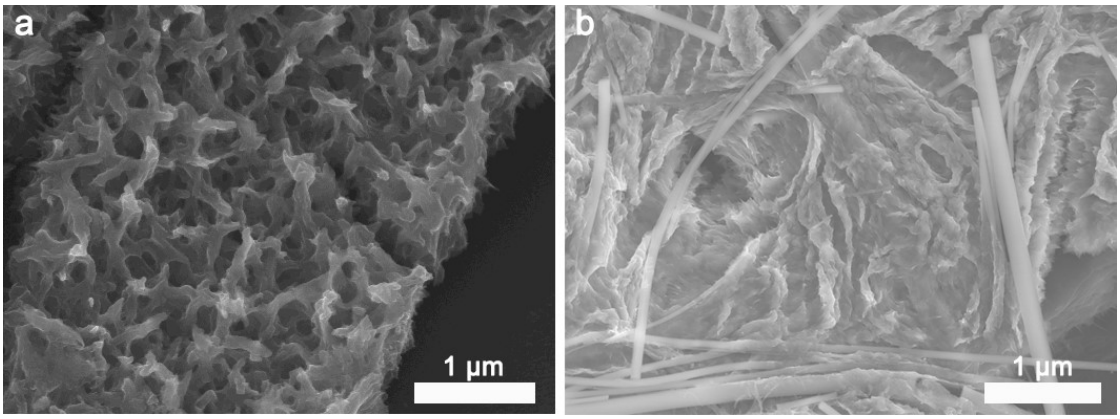

Fig. S12. SEM images of a) pristine VOH, and b) the electrode after 1000 cycles (VOH-1000).

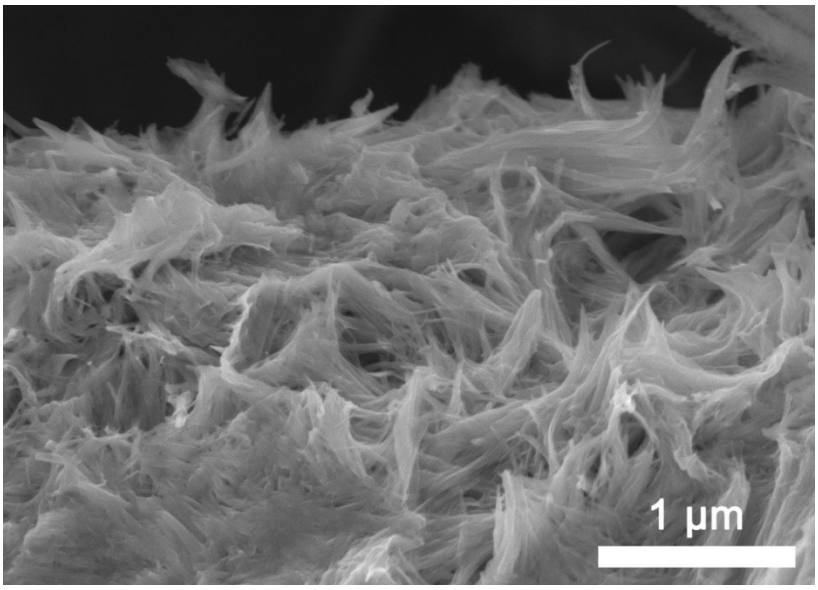

Fig. S13. SEM image of MgVOH electrode after 1000 cycles (MgVOH-1000).

Table S1. Calculated results of vibration for the Mg atom in MgVOH along different orientations

Orientations	Frequency/THz	Orientations	Frequency/THz
1	f = 112.217903	34	f = 13.376116
2	f = 111.163268	35	f = 13.143656
3	f = 111.077312	36	f = 12.164929
4	f = 110.505947	37	f = 11.403549
5	f = 108.749827	38	f = 11.269210
6	f = 108.465507	39	f = 11.106135
7	f = 107.955786	40	f = 10.230305
8	f = 107.605948	41	f = 9.739479
9	f = 106.300681	42	f = 9.092026
10	f = 104.825487	43	f = 8.841290
11	f = 103.196797	44	f = 8.381289
12	f = 102.455390	45	f = 8.029846
13	f = 96.487740	46	f = 6.855803
14	f = 87.196779	47	f = 6.814779
15	f = 49.362500	48	f = 6.781997
16	f = 48.936928	49	f = 6.536943
17	f = 48.251483	50	f = 6.098059
18	f = 48.161184	51	f = 5.829703
19	f = 47.479025	52	f = 5.678841
20	f = 47.056877	53	f = 4.860698
21	f = 46.778160	54	f = 4.695481
22	f = 27.166029	55	f = 4.561587
23	f = 24.920737	56	f = 4.457781
24	f = 23.552701	57	f = 4.271283
25	f = 22.330858	58	f = 4.174625
26	f = 19.898959	59	f = 4.077211
27	f = 19.726691	60	f = 4.007313
28	f = 18.203153	61	f = 3.522857
29	f = 16.625181	62	f = 3.417543
30	f = 16.356844	63	f = 3.119311
31	f = 15.260425	64	f = 3.035133
32	f = 14.711615	65	f = 0.963848
33	f = 13.534541	**66**	**f/i= 2.484736**